Communication

Essential Role of an Active-Site Guanine in *glmS* Ribozyme Catalysis

Daniel J. Klein, Michael D. Been, and Adrian R. Ferr-D'Amar

J. Am. Chem. Soc., **2007**, 129 (48), 14858-14859 • DOI: 10.1021/ja0768441

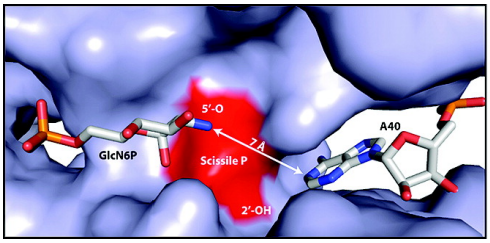

Position 40	GlcN6P	k_{obs} (min^{-1})
Guanine	−	~10^{-5}
Adenine	+	~10^{-5}
Guanine	+	>10

J|A|C|S
COMMUNICATIONS

Published on Web 11/09/2007

Essential Role of an Active-Site Guanine in *glmS* Ribozyme Catalysis

Daniel J. Klein,[†] Michael D. Been,[‡] and Adrian R. Ferré-D'Amaré*,[†]

Division of Basic Sciences, Fred Hutchinson Cancer Research Center, 1100 Fairview Avenue North, Seattle, Washington 98109, and Department of Biochemistry, Duke University Medical Center, Durham, North Carolina 27710

Received September 10, 2007; E-mail: aferre@fhcrc.org

The most common reaction catalyzed by ribozymes thus far discovered in nature is endonucleolytic cleavage. This transesterification reaction proceeds through an S_N2 mechanism and is initiated by attack of a 2′-OH on its adjacent phosphorus (Figure 1A). The transition state features a pentacoordinated phosphorus, and the products contain a 5′-OH and a 2′,3′-cyclic phosphate. A key challenge in understanding ribozyme function is to identify the contributions of RNA nucleobases to proton transfer and transition-state binding.[1]

Recently, activation of latent endonucleolytic cleavage activity in *glmS* messenger RNA by the metabolite glucosamine-6-phosphate (GlcN6P) was linked to negative control of *glmS* gene expression in *cis*[2]. A genetic switch results from minimizing the rate of self-cleavage in the absence of GlcN6P ($<10^{-5}$ min^{-1}, gene on), while maximizing the cleavage rate when bound to GlcN6P (>10 min^{-1}, gene off).[3,4] Crystal structures of the *glmS* ribozyme from *Thermoanaerobacter tengcongensis*[5,6] and *Bacillus anthracis*[7] in several functional states together with biochemical data[2,8,9] indicate that activation by GlcN6P does not require detectable conformational rearrangements of the ribozyme. Instead, the RNA provides a rigid scaffold that positions GlcN6P and the substrate of the cleavage reaction. The *glmS* ribozyme in the ligand-free state prior to cleavage closely aligns the 2′-OH nucleophile of residue A(−1) for S_N2 attack on the scissile phosphate.[5] Interestingly, the nucleophile is also within hydrogen-bonding distance of the N1 of nucleotide G40,[5,7] raising the possibility that this purine may act as a general base. However, the predicted rate of "spontaneous" cleavage (i.e., without chemical catalysis) at the scissile phosphate based on its "in-line fitness"[10] agrees well with experimentally determined rates for the *glmS* ribozyme in the absence of GlcN6P.[3,4] In addition, modification interference analysis of N2 and N7 of guanines did not identify a functional role for G40.[11] Therefore, current data argue that the role of the RNA, including G40, is limited to substrate positioning, while GlcN6P is exclusively responsible for accelerating the chemical step. However, this interpretation fails to explain the conservation of G40 in all known sequences of the *glmS* ribozyme.[12]

To investigate the importance of G40 to *glmS* ribozyme catalysis, we created a G40A mutation in the biochemically characterized *B. anthracis glmS* ribozyme.[6,7,13] The cleavage rate of this mutant in the presence of GlcN6P is $\sim 5 \times 10^{-5}$ min^{-1} (Figure 1B). In contrast, wild-type ribozyme cleaves at a rate of ~ 16 min^{-1} under identical conditions (Figure 1B). Therefore, mutation of position 40 (33 in *B. anthracis* numbering) to adenine abrogates most of the catalytic rate enhancement afforded by GlcN6P.

We considered the possibility that the importance of G40 to *glmS* ribozyme catalysis results from interactions in the transition state that require a guanine at this position. Other ribozymes have been

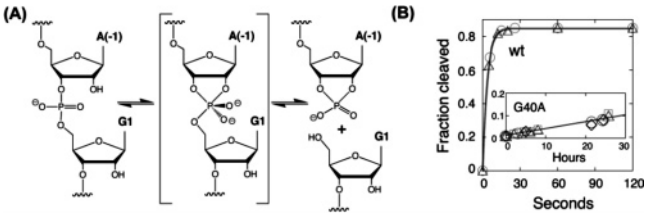

Figure 1. (A) Endonucleolytic cleavage reaction. (B) Cleavage of the *B. anthracis glmS* ribozyme. The data (symbols denote replicates) were fit to a first-order exponential to obtain k_{obs}. The inset shows that G40A mutation slows the rate of cleavage. Under the conditions of 0.5 mM GlcN6P, the k_{obs} for the G40A mutant ($5.1 \pm 1.2 \times 10^{-5}$ min^{-1}) was down 3×10^5-fold compared to the wild type (16.2 ± 0.3 min^{-1}).

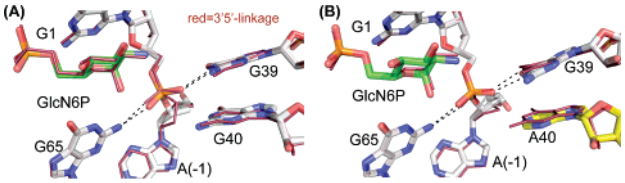

Figure 2. Comparisons of crystal structures of TSMs containing a 2′,5′ linkage at the scissile phosphate: (A) the wild type precleavage *glmS* ribozyme (thin, red) is superimposed on the wild type TSM (thick); (B) superposition of the TSMs of the wild type (thin, red) and the G40A mutant (thick).

proposed to catalyze endonucleolytic cleavage by binding the transition state more tightly than the precursor and product states, and this has been illustrated most notably for the hairpin ribozyme.[14] In those studies, crystal structures were determined using several different transition state mimics (TSMs), including a vanadate complex[14,15] and a 2′,5′-linked scissile phosphate RNA inhibitor.[15] In the case of the *glmS* ribozyme, assembly of the vanadate complex requires that the product state ribozyme bind adenosine in order to mimic nucleotide A(−1), the only nucleotide 5′ of the scissile phosphate that is contacted by the ribozyme.[5,7] Presumably as a result of weak affinity for adenosine of the ribozyme, vanadate failed to assemble into a TSM in crystals of the *T. tengcongensis glmS* ribozyme (data not shown). To mimic the transition state, we instead employed an RNA inhibitor containing 3′-deoxy-A(−1) covalently linked to residue G1 via a 2′,5′ linkage (Figure 2). This inhibitor has been shown to mimic the transition state with respect to the orientation of the nonbridging phosphate oxygens.[15] We determined crystal structures of the wild type and G40A mutant *T. tengcongensis glmS* ribozymes complexed with this RNA inhibitor at 3.0 and 2.7 Å resolution, respectively. GlcN6P was bound in both structures. The wild type ribozyme revealed little difference in the orientation of the nonbridging phosphate oxygens as compared to that observed for the wild type ribozyme in the pre-cleavage state (Figure 2A). In the structure of the G40A mutant bound to the 2′,5′-linked RNA inhibitor, the scissile phosphate adopts this same conformation (Figure 2B). In all of these structures,

[†] Fred Hutchinson Cancer Research Center.
[‡] Duke University.

10.1021/ja0768441 CCC: $37.00

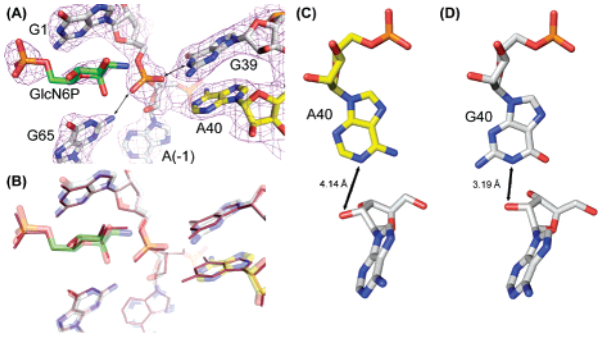

Figure 3. (A) Active site of the G40A mutant of the *T. tengcongensis glmS* ribozyme superimposed on a $2|F_o| - |F_c|$ electron density map (2.7 Å resolution); (B) superposition of the active site structures of G40A (thick) and wild-type (thin, red) *glmS* ribozymes; (C and D) interaction between the 2′-OH of A(−1) and A40 in the mutant (C) or G40 in the wild type ribozyme (D).

putative hydrogen bonds from the nonbridging oxygens of the scissile phosphate are maintained to the N1 of G39 and the N2 of G65. Assuming the 2′,5′-linked RNA inhibitor mimics the transition state of the *glmS* ribozyme, it appears that the scissile phosphate is held rigidly in place upon progression to the transition state. Therefore, structures of this TSM bound to the *glmS* ribozyme do not indicate an obvious mechanism by which tighter binding to the transition state could be achieved. Moreover, structural differences between TSM complexes of the wild type and of the G40A mutant ribozymes are undetectable, suggesting that G40A mutants are inactive for reasons other than disruption of the transition-state geometry.

We next considered the possibility that loss of activity in *glmS* ribozymes containing the G40A mutation could result from disruption of GlcN6P binding or the in-line conformation of reactive groups in the precleavage state. To examine this possibility at the structural level, we determined a crystal structure of the G40A mutant ribozyme complexed with GlcN6P and an RNA substrate containing a 2′-OH group at A(−1). Under these conditions, wild-type *glmS* ribozymes undergo cleavage in the crystalline state,[5] as indicated by loss of electron density for residue A(−1). However, crystals of the G40A mutant yielded electron density maps at 2.7 Å resolution that showed clear density for A(−1) (Figure 3A). In the structure of the mutant, the active site adopts a conformation that is nearly identical to that of the wild-type ribozyme complexed with the inhibitor glucose-6-phosphate[5] (rmsd of C1′ atoms of the active site residues = 0.28 Å) (Figure 3B). Despite the mutation, the 2′-OH of A(−1) is still positioned for S_N2 attack relative to the phosphorus and the 5′-oxygen leaving group of G1. Strikingly, GlcN6P is bound in the same position it occupies in the wild type ribozyme (Figure 3B).[6,7] Therefore, reduction of the catalytic rate by $\sim 10^5$ in the mutant ribozyme is not due to disruption of the conformation of reactive groups or of GlcN6P binding in the precleavage state. Unexpectedly, the structure demonstrates that an in-line conformation of reactive groups and precise positioning of GlcN6P together are not sufficient for effective catalysis.

Why then do *glmS* ribozymes containing the G40A mutation fail to cleave at rates similar to those observed for the wild-type ribozyme? Upon close inspection, one difference we noted in the active site was a subtle change in the disposition of the A40 nucleobase relative to the ribose of A(−1) (Figure 3C). This difference weakens the inferred hydrogen bond between the 2′-OH of A(−1) and the N1 of A40 (4.14 Å), relative to that observed for G40 (3.19 Å) (Figure 3D). Assuming pK_a values of ~3.5 and ~9.5 for the N1 nitrogens of A40 and G40, respectively, these results suggest that donation of a hydrogen bond by this group to the 2′-OH nucleophile is critical for structure and presumably catalysis. Alternatively, these results are consistent with a requirement that the N1 of G40 be close enough to abstract a proton from the 2′-OH nucleophile. In either case, the data uncover a pronounced effect of the N1 of G40 on the ability of the coenzyme GlcN6P to perform its catalytic role. We conclude that the N1 of G40 is just as important for *glmS* ribozyme cleavage as the 2-amine of GlcN6P, the proposed[5] general acid and electrostatic catalyst.

In summary, we have demonstrated that mutation of the guanine at position 40 to adenine abrogates *glmS* ribozyme catalysis, although substrate and coenzyme positioning and transition state binding appear unaffected. In contrast, mutation of G8[16] and C75[17] of the hairpin and HDV ribozymes, respectively, results in catalytic impairment that could be explained by structural disruption of their active sites.[16,18,19] The *glmS* ribozyme requires G40 and GlcN6P together for catalysis; either in isolation provides only negligible rate acceleration. This observation supports a mechanism in which the N1 of G40 becomes an effective general base only upon binding of GlcN6P to the ribozyme. Likewise, our structure of the G40A mutant supports a mechanism in which the 2-amine of GlcN6P requires G40 to become an effective general acid. Therefore, our data reveal strong interdependence between GlcN6P and G40.

Acknowledgment. We thank S.R. Wilkinson for the *B. anthracis* ribozyme constructs and the staff at the Advanced Light Source. A.R.F. is a Distinguished Young Scholar in Medical Research of the W. M. Keck Foundation. D.J.K. is a Damon Runyon Fellow (Grant DRG-1863-05). Also supported by grants from the NIH (Grant GM63576 to A.R.F. and Grant GM47233 to M.D.B.) and the W. M. Keck Foundation. Coordinates and structure factors have been deposited in the Protein Data Bank (3b4a, 3b4b, and 3b4c).

Supporting Information Available: Experimental methods. This material is available free of charge via the Internet at http://pubs.acs.org.

References

(1) Bevilacqua, P. C.; Yajima, R. *Curr. Opin. Chem. Biol.* **2006**, *10*, 455−464.
(2) Winkler, W. C.; Nahvi, A.; Roth, A.; Collins, J. A.; Breaker, R. R. *Nature* **2004**, *428*, 281−286.
(3) McCarthy, T. J.; Plog, M. A.; Floy, S. A.; Jansen, J. A.; Soukup, J. K.; Soukup, G. A. *Chem. Biol.* **2005**, *12*, 1221−1226.
(4) Roth, A.; Nahvi, A.; Lee, M.; Jona, I.; Breaker, R. R. *RNA* **2006**, *12*, 607−619.
(5) Klein, D. J.; Ferré-D'Amaré, A. R. *Science* **2006**, *313*, 1752−1756.
(6) Klein, D. J.; Wilkinson, S. R.; Been, M. D.; Ferré-D'Amaré, A. R. *J. Mol. Biol.* **2007**, *373*, 178−189.
(7) Cochrane, J. C.; Lipchock, S. V.; Strobel, S. A. *Chem. Biol.* **2007**, *14*, 97−105.
(8) Hampel, K. J.; Tinsley, M. M. *Biochemistry* **2006**, *45*, 7861−7871.
(9) Tinsley, R. A.; Furchak, J. R.; Walter, N. G. *RNA* **2007**, *13*, 468−477.
(10) Soukup, G. A.; Breaker, R. R. *RNA* **1999**, *5*, 1308−1325.
(11) Jansen, J. A.; McCarthy, T. J.; Soukup, G. A.; Soukup, J. K. *Natl. Struct. Mol. Biol.* **2006**, *13*, 517−523.
(12) Barrick, J. E.; Corbino, K. A.; Winkler, W. C.; Nahvi, A.; Mandal, M.; Collins, J.; Lee, M.; Roth, A.; Sudarsan, N.; Jona, I.; Wickiser, J. K.; Breaker, R. R. *Proc. Natl. Acad. Sci. U.S.A.* **2004**, *101*, 6421−6426.
(13) Wilkinson, S. R.; Been, M. D. *RNA* **2005**, *11*, 1788−1794.
(14) Rupert, P. B.; Massey, A. P.; Sigurdsson, S. T.; Ferré-D'Amaré, A. R. *Science* **2002**, *298*, 1421−1424.
(15) Torelli, A. T.; Krucinska, J.; Wedekind, J. E. *RNA* **2007**, *13*, 1052−70.
(16) Salter, J.; Krucinska, J.; Alam, S.; Grum-Tokars, V.; Wedekind, J. E. *Biochemistry* **2006**, *45*, 686−700.
(17) Ke, A.; Zhou, K.; Ding, F.; Cate, J. H.; Doudna, J. A. *Nature* **2004**, *429* (6988), 201−205.
(18) Das, S. R.; Piccirilli, J. A. *Nat. Chem. Biol.* **2005**, *1*, 45−52.
(19) Strobel, S. A. *Nat. Chem. Biol.* **2005**, *1*, 5−6.

JA0768441